XPS MultiQuant

for Windows

Application Examples

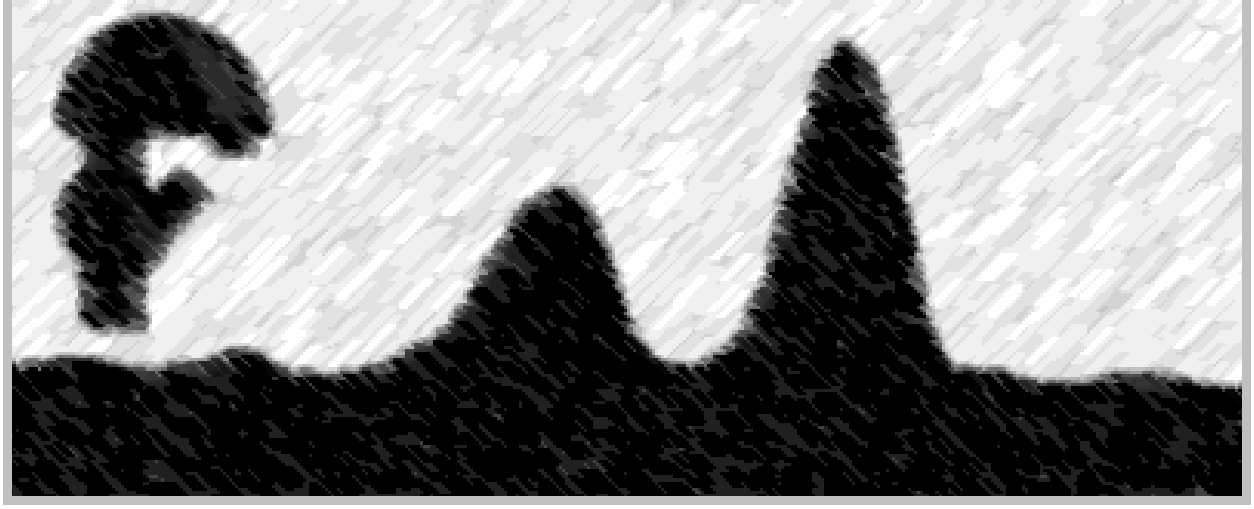

Statuette of Imhotep

The Egyptian Collection of the Museum of Fine Arts in Budapest has a small statue of Imhotep. Imhotep was an Egyptian scientist (later he was respected as a god), he built the first pyramid for pharaoh Djoser in Saqqara.

It was reasonable assumed that various parts of the statuette were made of different alloys thus samples from of several parts were analysed. The quantity of the available samples was limited and it had to be preserved for other investigations as well.

The chart shows the metallic composition of the different samples while other elements (oxygen, carbon, etc.) are omitted. One the basis of the analyses, the samples can be categorised in two groups: lead containing (footstool) and lead free (chair, chairbase) alloys.

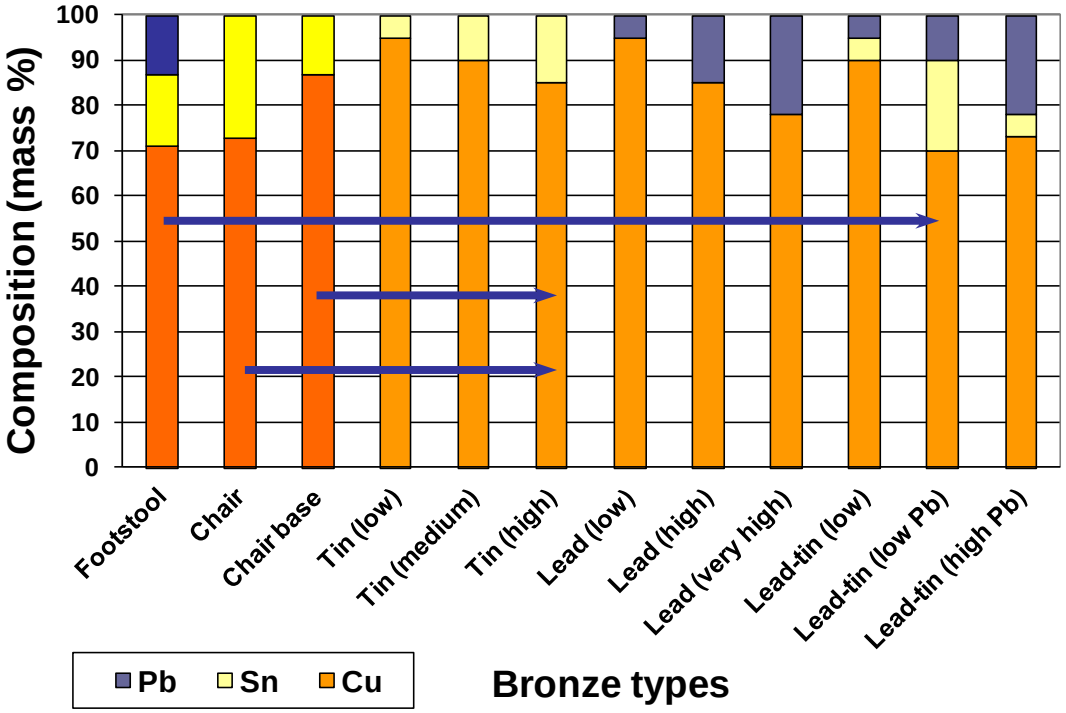

Bronze alloys are categorised by the tin and lead content in the literature. By the quantitative analysis the materials of the statuette can be assigned as “tin-bronze with high tin content” and “lead-tin-bronze with low lead content”. The questions whether the various parts of the statuette originally belonged together or nor, whether they come from the same workshop or not, and what are the conclusions on age determination cannot be fully answered. Chemical composition data are available only for a limited number of accurately dated bronze objects. In any case, our results still contribute to the clarification of the genetics of the bronze statuette.

M. Tóth, I. Bertóti, M. Mohai, I. Fórizs, I. Vozil: Material Analysis of the Bronze Statuette of Imhotep,
Bulletin du Musée Hongrois des Beaux-Arts 95 (2001) 35.

Depth Profile – Handling of Multistep Series

These XPS spectra were recorded on an electrical contact prepared on a silicon wafer from titanium and silver. The sample was heat-treated causing diffusion of the components. The upper layers were oxidised and the top surface was contaminated by carbon. Ion etch series were performed by 2 keV Ar^+ ions in 2 min steps.

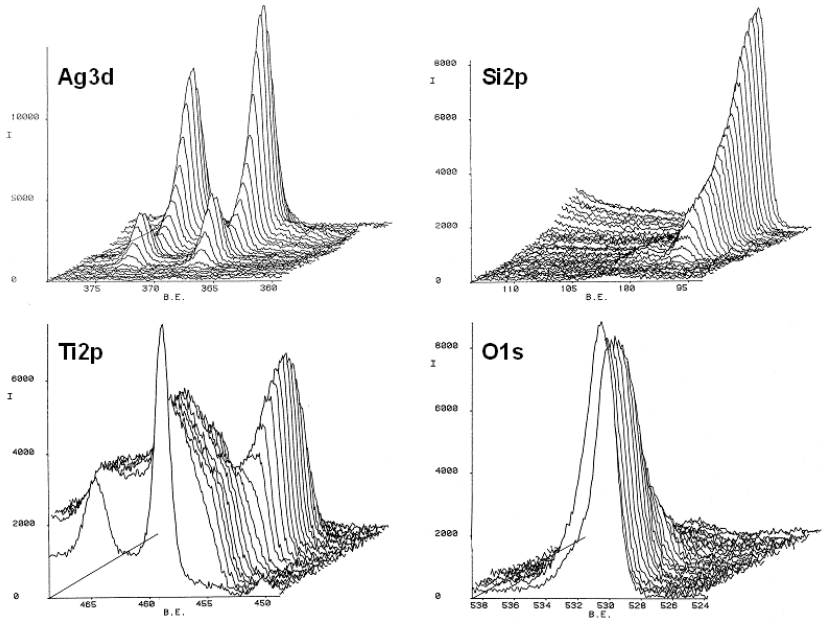

The ion etch depth profile reflects the changes seen on the previous figure. Beside the intensity (height) changes of the lines consider alterations in FWHM as well; this explains the shallower concentration differences visible in the Ti profile. The reduction of the system can be seen from not only the chemical shift changes but the decreasing oxygen balance, as well.

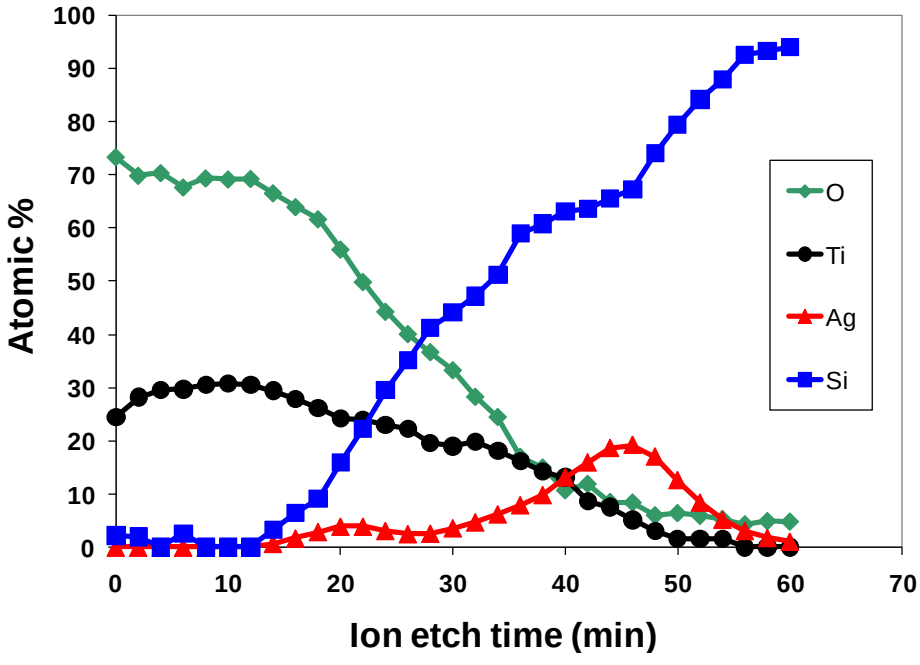

I. Bertóti, A. Tóth, M. Mohai: Szilícium napelemeken kialakított fémkontaktusok XPS vizsgálata.
(XPS Investigation of Metal Contacts Prepared on Silicon Solar Cells.)
Research report (unpublished).

Using of Oxygen Balance

Cr-O-Si cermet films are widely applied in microelectronics devices. Such layers were prepared by RF-sputtering of a Cr:O:Si target with a nominal atomic ratio of 1:1:1 onto thermally oxidised silicon wafers. XP spectra of the characteristic lines (Cr2p, Si2p, O1s, C1s) were recorded. Ion bombardments were performed by 2 keV Ar^+ ions. Composition, expressed in *Oxide molar ratio*, was calculated for assumed combinations: **Cr_2O_3+SiO_2**, **Cr_2O_3+Si** and **Cr+SiO**. The *Oxygen balance*, the ratio of the measured and calculated (according to the assumed "stoichiometric" formula) oxygen concentrations, are depicted on the figure as a function of the bombardment time.

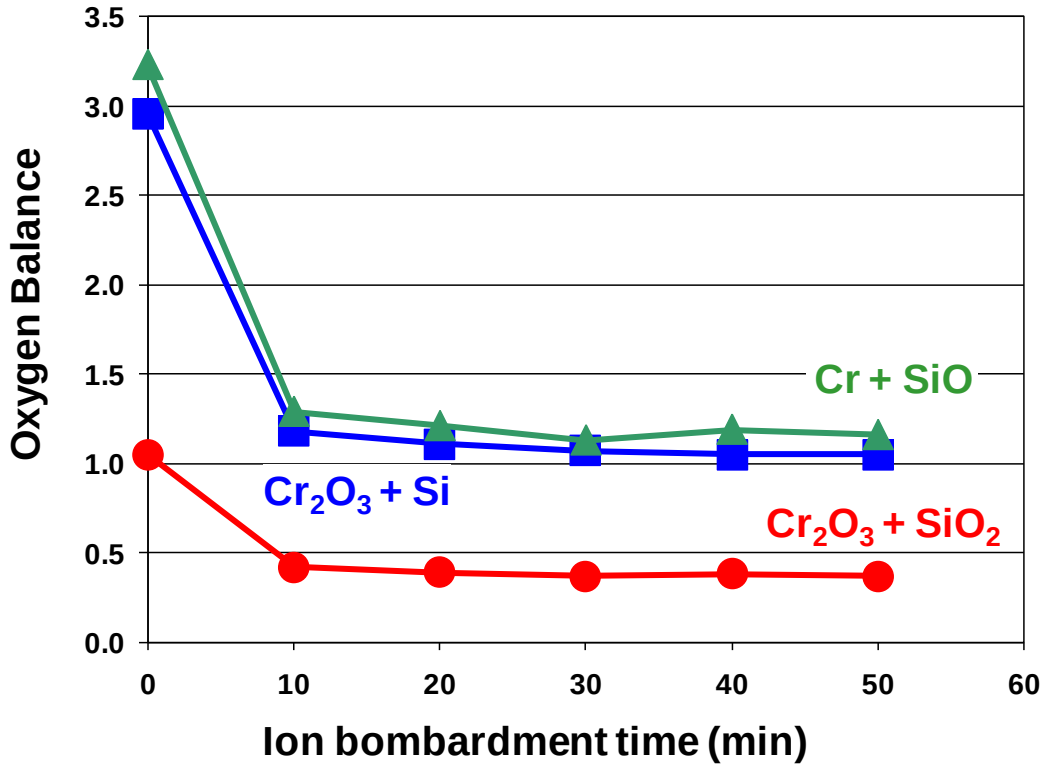

The chart revealed that the top surface is totally oxidised, i.e., $O_{obs}/O_{cal} \approx 1$ for the assumed Cr_2O_3+SiO_2. After 10 min bombardment, the top layer is removed and the former composition gives unrealistic oxygen deficiency. The composition of the layer is close to either of the Cr_2O_3+Si or Cr+SiO (or also CrO+Si) supposed structures. Further bombardment does not change the composition. Chemical shifts of the photoelectron lines will determine the correct chemical structure but this method can reduce the choice, discard unrealistic combinations and by this back the peak decomposition procedure.

I. Bertóti, A. Tóth, M. Mohai, R. Kelly, G. Marletta: Effect of Ion Bombardment on Cr-Si-O Layers: An X-ray Photoelectron Spectroscopic Study, *Thin Solid Films* 241 (1994) 211-217.

I. Bertóti, A. Tóth, M. Mohai, R. Kelly, G. Marletta: He^+ and Ar^+ Bombardment Induced Chemical Changes in Cr-O-Si Layers, *Nucl. Instrum. Methods B* 116 (1996) 200.

Corrections for Carbonaceous Contamination

XPS data were measured on a thermally oxidised Si wafer. The sample was totally oxidised and no elemental silicon could be detected. It was treated by low-pressure oxygen plasma to remove residual carbon and reach the stoichiometric Si:O = 1:2 ratio. After measuring the clean state of the sample, hydrocarbon contamination of increasing thickness was deposited by casting of polystyrene from benzene solution in subsequent steps.

The compositions of the samples (atomic ratio) were calculated with different contamination correction methods. Without application of such corrections a substantial error is introduced.

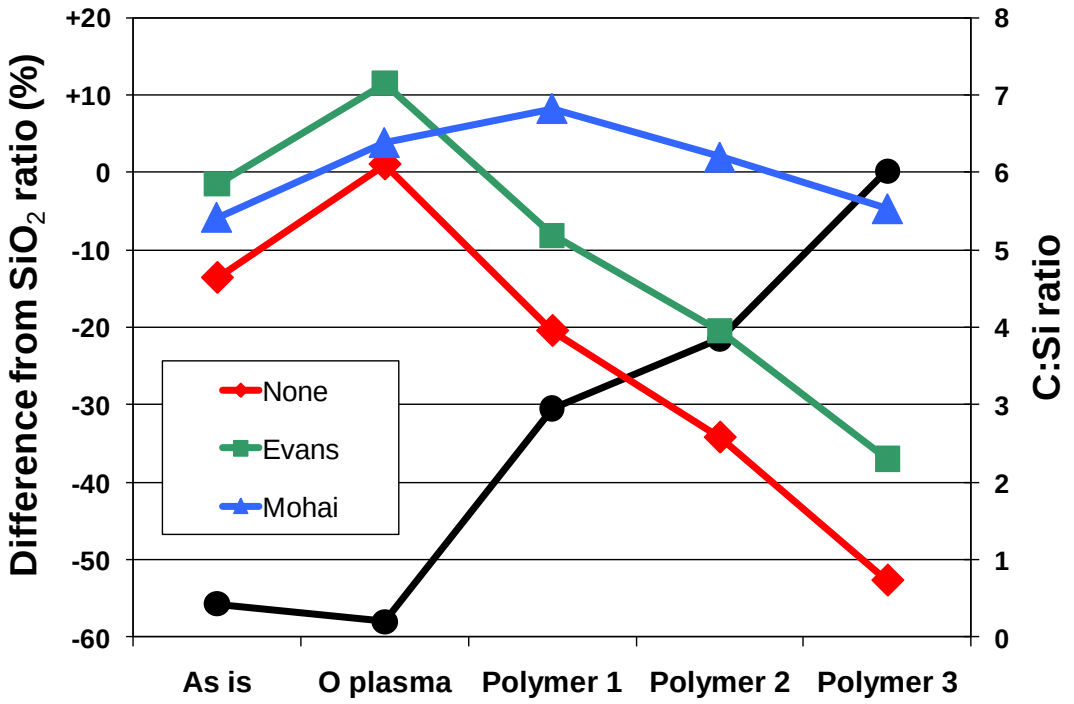

When no correction is applied, only the clean (O plasma) sample gives the correct composition. The method of Evans is optimised for the 'averrage' contamination (As is) thus the clean sample is overcorrected. Mohai's method supplies the composition within the ±10 % difference range for low and high levels of contamination.

M. Mohai, I. Bertóti: Correction for Surface Contaminations in XPS: A Practical Approach, in: *ECASIA 95* (Eds. H. J. Mathieu, B. Reihl, D. Briggs), John Willey & Sons, Chichester-New York-Brisbane-Toronto-Singapore (1995), p. 675.

M. Mohai: *XPS MultiQuant for Windows User's Manual* (1999).

Study of Silylated Glass Surface

The soda-lime glass samples were etched with hydrochloric acid and heat treated 550 K in air. Then samples were silylated was with hexamethyl-disiloxane vapour in a sealed glass ampoule.

The acid treatment performed under moderate conditions leads to the complete depletion of Na, K, Ca and a partial depletion of Al to a depth far beyond the detection limit of XPS. The heat treatment did not stimulate reappearance of K and Ca in the surface layers to levels above the detection limit.

Two types of carbon atoms were found: the hydrocarbon type from the methyl groups and a H-C-O type contamination. Two types of oxygen and silicon could be distinguished. The smallest peaks can be identified as those originating from the supposed $(CH_3)_3$-Si-O type surface species, while the larger ones originate from the oxygen and silicon atoms of the glass surface network.

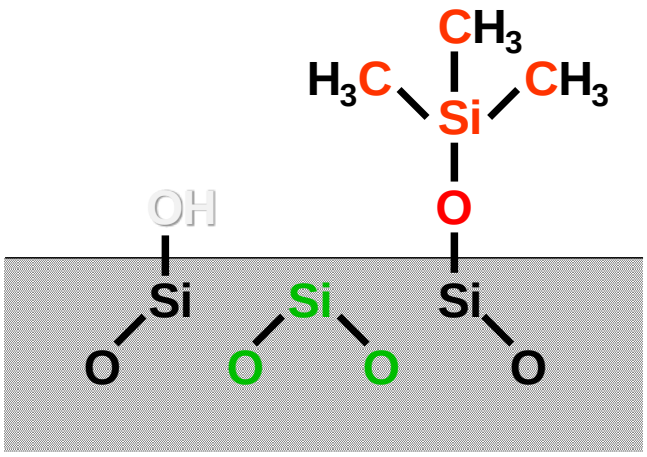

Peak	Binding energy *(eV)*	Composition *(atomic %)*		Origin
C1s	286.1	2.4		contamination
	284.1	11.5	(3)	$-CH_3$
O1s	533.2	46.7	(2)	Si-O-Si, Si-OH
	531.5	3.6	(1)	$(CH_3)_3$Si-O-
Si2p	103.8	27.2	(1)	Si-O-Si, Si-OH
	102.2	3.9	(1)	$(CH_3)_3$Si-

As it can be seen, the atomic % values for the $(CH_3)_3$SiO-group show an excellent consistency with the expected 3:1:1 ratio. The binding energy values are in good accordance with the literature. The ratio of the corresponding bulk Si and O atoms is also close to 2, which means that OH groups can hardly be found on the silylated surface.

I. Bertóti, M. Mohai, M. Révész, G. Alexander: Surface Composition of Glasses: Modifications Induced by Chemical and Heat Treatments, *Vacuum* 37 (1987) 129.

Langmuir-Blodgett Film Study

Lead arachidate Langmuir-Blodgett (LB) films with two monomolecular layers were deposited on trimethyl-silylated glass substrates and studied by X-ray Photoelectron Spectroscopy. XP spectra of the O1s, C1s, Pb4f and Si2p lines were recorded. The completeness of the salt formation was assessed by the normalised intensity ratio of the carboxylic (–COO–) type carbon component with C1s B.E. at about 288.5 eV and that of the Pb cation.

The *Layers-on-Plane* model was applied with the following arrangement: the Pb-arachidate monolayer was considered as two sublayers due to the dissimilar nature of the two parts of the molecule. The physical constants (molecular mass, density, IMFP) of the octadecane ($C_{18}H_{38}$) and the lead acetate ($Pb(COOCH_3)_2$) were used for the hydrocarbon chain and the hydrophilic part of the molecule, respectively. The contribution of the silyl groups was neglected.

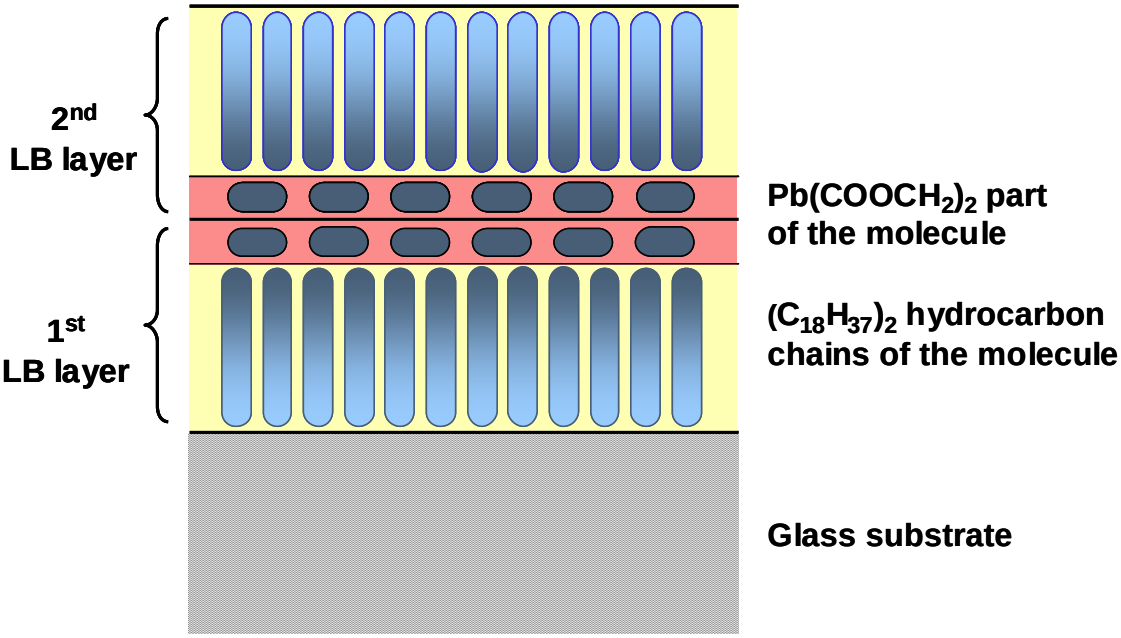

In the program a double arachidate layer was implemented by three sublayers, as shown in the figure; and one or two of this structure were applied for the calculation of the 2L and 4L samples, using the *Multilayers* attribute.

The calculated thickness of the lead arachidate monolayer was 28.8 Å, while the reported value in the literature is 28 Å. The realistic thickness ratio of the two sublayers justifies the presence of the Y-type layer structure.

M. Mohai, É. Kiss, A. Tóth, J. Szalma, I. Bertóti: Preparation and Characterisation of Langmuir-Blodgett Type Arachidate Films, *Surf. Interface Anal*. 34 (2002) 772.

Using of Spherical Model: Silicon Nitride Nanopowder

Silicon nitride nanodisperse powder, synthesised in RF thermal plasma, was aged in air of 80 % relative humidity and also in dry air. This powder consisted of nearly spherical particles with 400 Å average diameter. The structure of the particles was assumed as follows: a core of Si_3N_4 is surrounded by a SiO_2 layer and a carbonaceous contaminant layer.

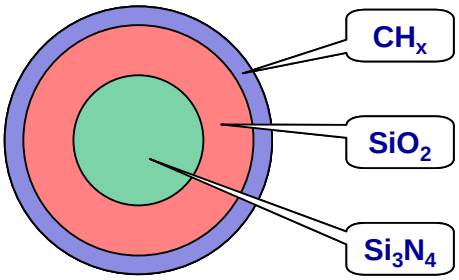

Intensity ratios of the characteristic lines (Si2p, N1s, O1s, C1s) were calculated using the *Layers-on-Sphere* model and fitted to the measured values.
Results clearly demonstrate the fast development of the oxidised layer in the humid atmosphere while the thickness of the contaminant layer is practically unchanged.

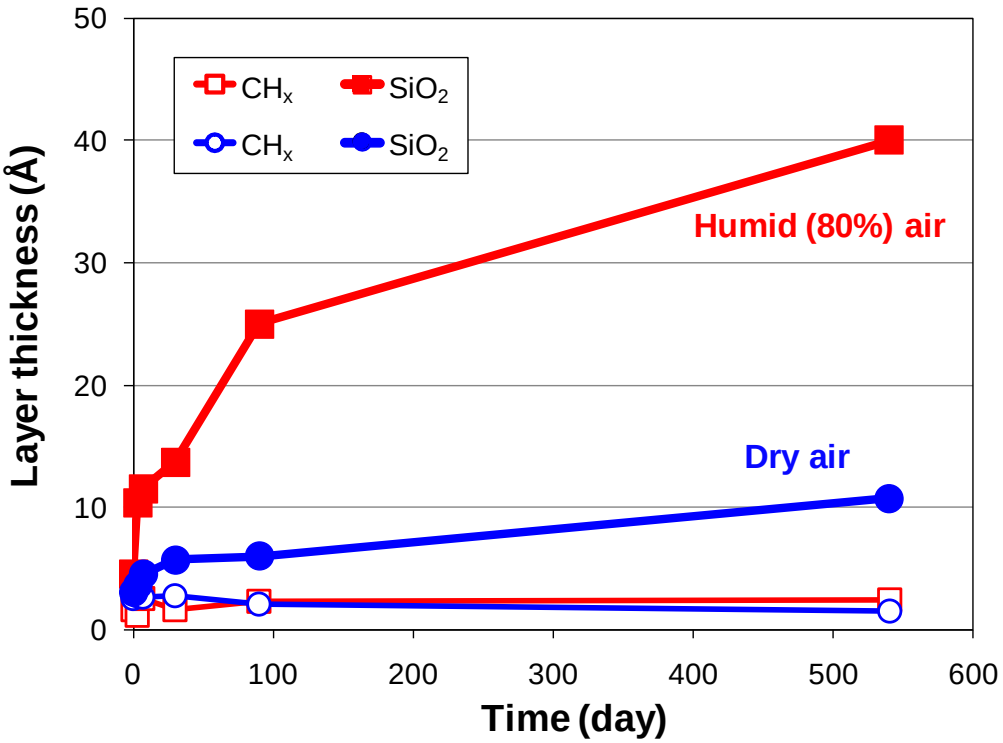

Increasing of the thickness of the SiO_2 layer on the Si_3N_4 particles during long term ageing

J. Szépvölgyi, I. Mohai, J. Gubicza: Atmospheric Ageing of Nanodisperse Silicon Nitride Powders,
J. Mat. Chem. 11 (2001) 859.

Testing of Cylindrical Model: Aluminium Foil

A flat aluminium foil was measured at 0 and 60° take-off angles and the thickness of the oxide and contaminant layers were calculated by the *Layers-on-Plane* model. Subsequently the same foil was spooled, to form tiny cylinders, while preserving the same thickness of the oxide layer. Several of these cylinders were tightly assembled by sticking them to a flat sample holder and measured at 0° take-off angle with FAT and FRR spectrometer modes.

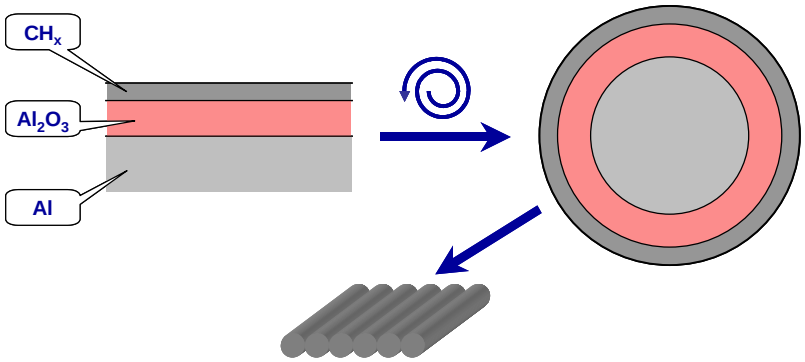

The layer thickness was calculated by the *Layers-on-Cylinder* model, resulting the same thickness for the oxide layer as done by the *Layers-on-Plane* model for the flat arrangement. During the sample manipulation, the thickness of the contamination layer inevitably increased slightly but as it was taken into account, it has not altered the calculated thickness of the oxide layer.

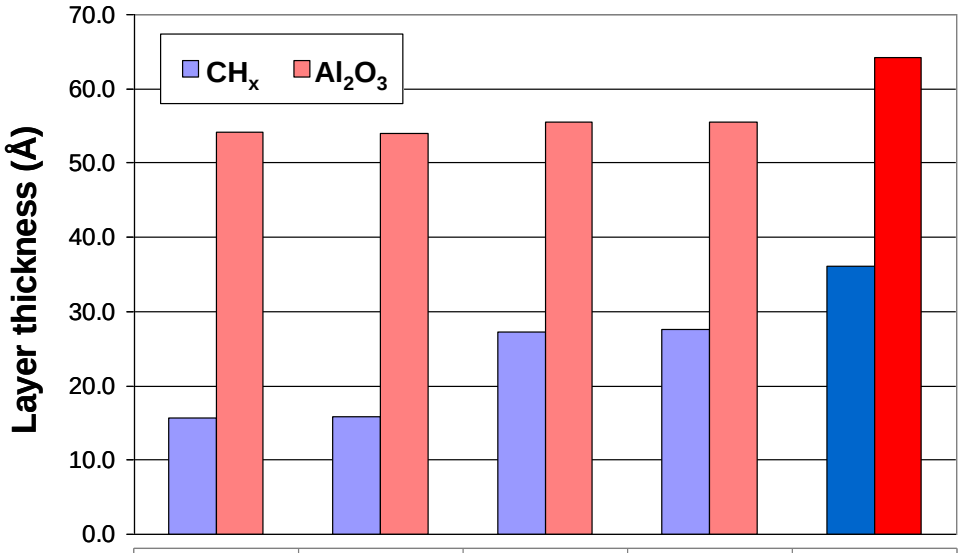

Sample shape	flat	flat	cylinder	cylinder	cylinder
Quantification model	planar	planar	cylindrical	cylindrical	planar
Spectrum mode	FAT	FAT, 60°	FAT	FRR	FAT

The validity of the proposed calculation is approved by the excellent agreement of the thickness values of the oxide layers. Conversely, when the planar model was applied to the cylindrical samples, the thickness of the layer was overestimated by more than 15 %. This way of testing of the model is based on relative comparison and not perturbed by any uncertainties of other terms of the calculations, e.g., cross section, IMFP, analyser transmission, etc.

M. Mohai, I. Bertóti: Calculation of Overlayer Thickness on Curved Surfaces Based on XPS Intensities,
Surf. Interface Anal. 36 (2004) 805.

Ion Bombardment of Oxides

The behavior of oxides bombarded by chemically neutral ions, i.e., noble gas ones, is widely documented in connection with ion-beam assisted layer deposition or removal, as well as with sputter depth profiling. Oxides tend to loose oxygen preferentially, even of oxides declared to be stable under nobel gas atom (or ion) impact.

Bombardment sequences of $Ar^+ - N_2^+ - Ar^+$ have been applied to SiO_2 target. The steady state concentrations are shown in the next figure. More oxygen is lost when bombarded by N_2^+ as compared to Ar^+. The N1s peak can be assigned to nitride-type nitrogen

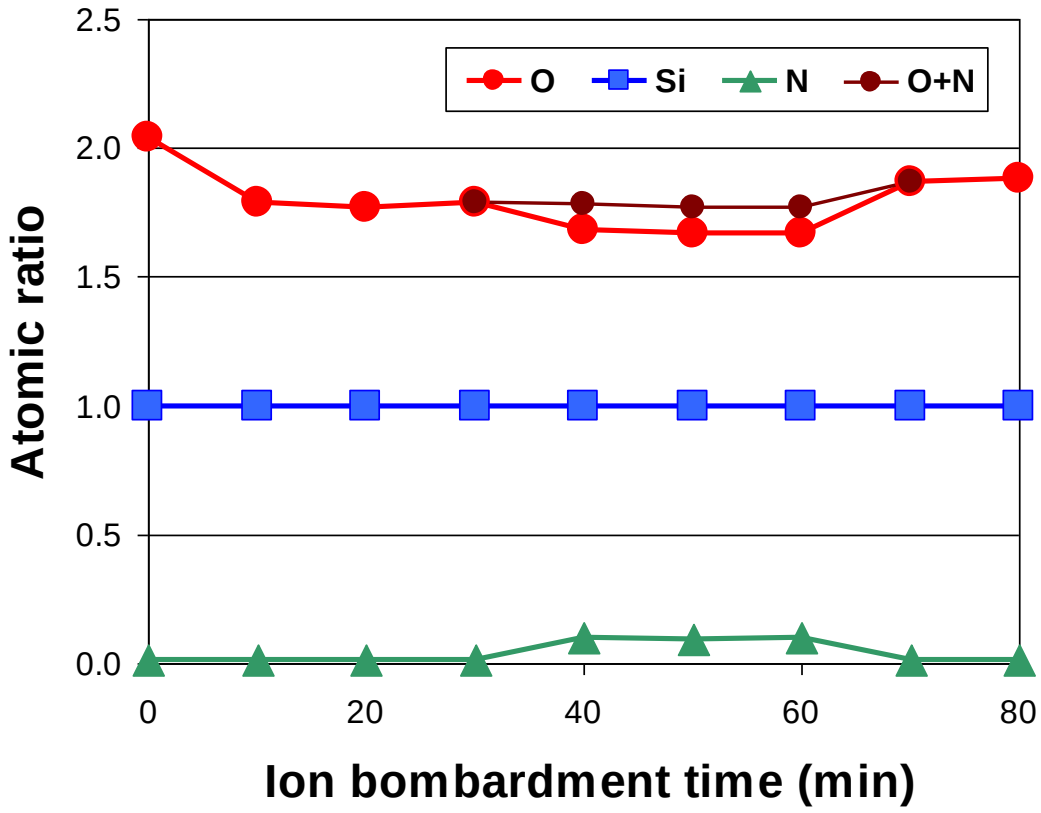

The observed approx. 1:1 replacement of (excess) oxygen by nitrogen is nonsense in chemical sense, considering normal valence states. The observed experimental fact can be interpreted for the case of SiO_2 in the following way:

For accomodation of a nitrogen atom to a nitride type environment (as in Si_3N_4) it needs three neighbouring silicon atoms with unsaturated (dangling) bonds. This is, however, must be a highly energetic short living state, undergoing some kind of relaxation (e.g., by oxygen recoils), that is why we cannot detect them after Ar^+ bombardment. This type of reaction sites can be created by N projectiles, when they produce an oxygen vacancy next to an already existing one with a simultaneous replacement. That is why 1:1 replacement is observed, although the built-in N realises in fact three bonds (according to the observed chemical shift of the N1s line).

I. Bertóti, R. Kelly, M. Mohai, A. Tóth: A Possible Solution to the Problem of Compositional Change with Ion-bombarded Oxides, *Surf. Interface Anal.* 19 (1992) 291.

I. Bertóti, R. Kelly, M. Mohai, A. Tóth: Response of Oxides to Ion Bombardment: The Difference between Chemically Inert and Reactive Ions, *Nucl. Instrum. Methods B* 80/81 (1993) 1219.

Nitrogen-PBII Modification of Ultra-High Molecular Weight Polyethylene

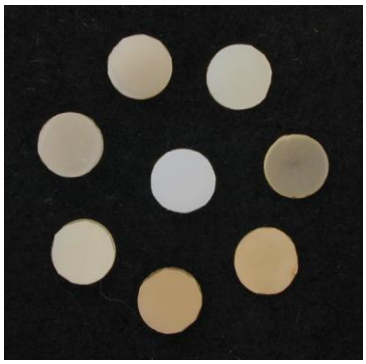

Wear and wear debris induced limitation of the service life of ultrahigh molecular weight polyethylene hip and knee joint components is of great concern at the biomedical implant application of this material. Numerous attempts have been made for improving the wear properties of PE, including *plasma based ion implantation* (PBII).

Plasma based ion implantation of nitrogen was performed on mechanically polished UHMWPE model samples by applying low pressure N_2 plasma with 15–30 kV pulses. Surface compositional and structural alterations were investigated by XPS.

The surface composition of some representative samples is shown in the figure. As seen, in addition to the implanted nitrogen, relatively large amount of oxygen was measured on samples kept in vacuum for 30 minutes after the implantation (Samples 1-3). In contrast to this, very low level of oxygen but much higher N content was measured for those samples 'cooled down' after the PBII treatment in N_2 plasma (Sample 4). Storing the samples in ambient for long period led to further increase of oxygen. A 'light' Ar^+ ion etch (1.5 keV, <1 μA/cm^2, 5 min) removed almost completely the oxygen.

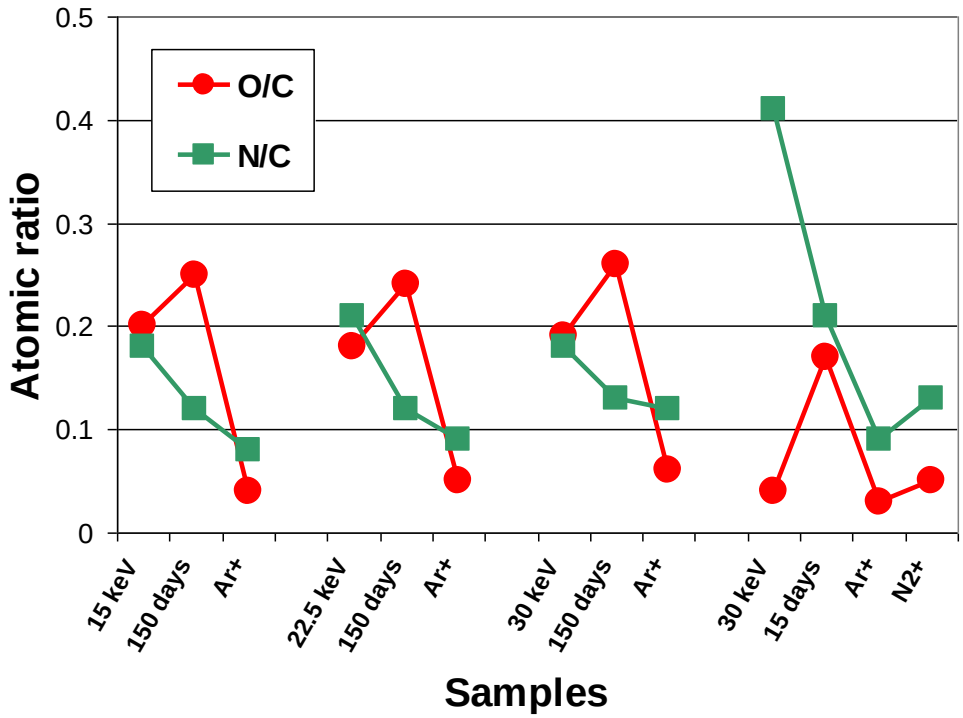

From the above, it can be concluded that the active sites created by the PBII treatment are recombined either by oxygen (and water) in the one or by nitrogen in the other case of the post-treatment. Another conclusion is that the majority of oxygen is situated at the near surface region of the samples. Water chemisorption may be the cause of the further increase of oxygen at storage in ambient.

I. Bertóti, M. Mohai, A. Tóth, T. Ujvári: Nitrogen-PBII modification of ultra-high molecular weight polyethylene: Composition, structure and nanomechanical properties, *Surf. Coat. Technol.* 201 (2007) 6839.

Zinc Hydroxystannate-Coated Fillers

Zinc hydroxystannate ($Zn[Sn(OH)_6]$, ZHS)-coated fillers are novel flame retardant and smoke suppressant additives for polymeric materials. The application of ZHS coating to various hydrated inorganic fillers, in particular aluminium hydroxide or magnesium hydroxide, allows significant reduction to be made in the overall filler loading, with no loss in their flame retardant properties.

Based on the lamelliform morphology of the particles, for quantification of the coated samples the *Islands-on-Plane* model was applied. It is supposed that the planar substrate is covered by islands of ZHS, and this system is covered uniformly by the ubiquitous thin carbonaceous contamination layer, CH_x.

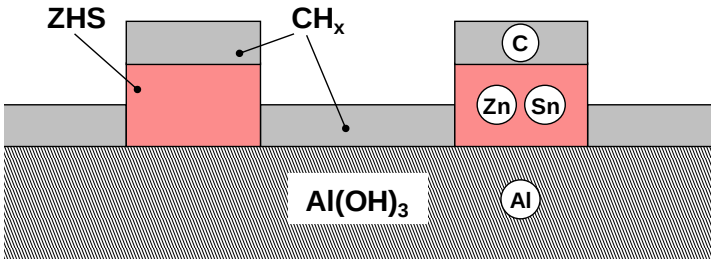

In the next figure the layer thickness of ZHS versus surface coverage is depicted. When the bulk concentration of ZHS is higher than 10 %, the slope of the dependence seems to become very steep, suggesting that at high bulk concentrations of the ZHS coating, it is mainly the layer thickness, which tends to increase and not the degree of coverage.

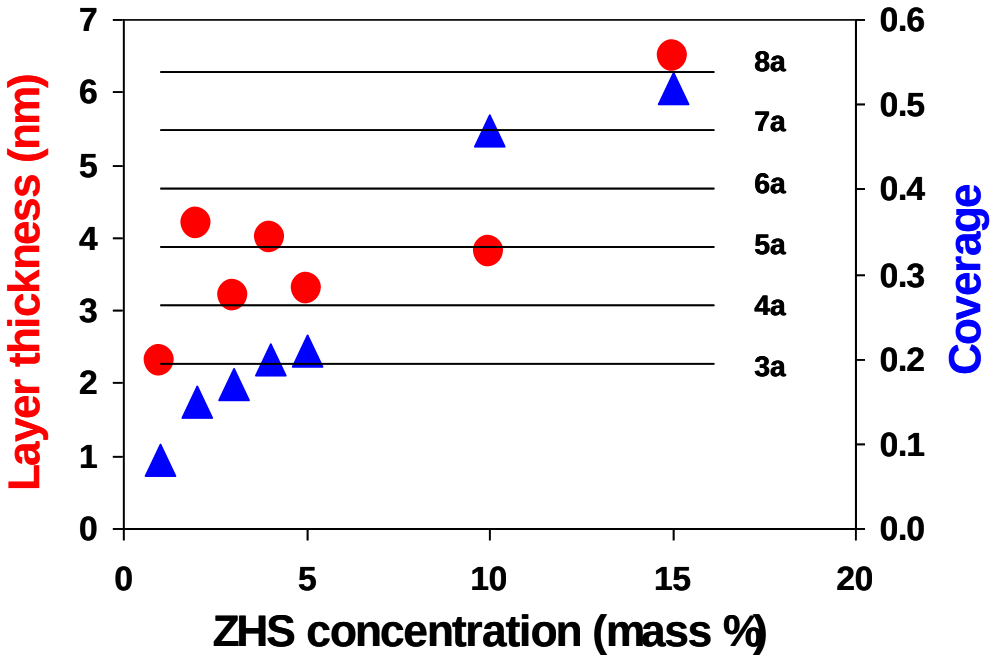

According to the ASTM cards, ZHS has a cubic cell with a lattice parameter a = 0.772 nm (ASTM 33-1376) or 0.78 nm (ASTM 20-1455). It seems that the measured layer thickness values correspond to multiples of the lattice parameter, implying that with the increase of coverage the number of monolayers increases from 3 to 8 in the experimental range studied.

M. Mohai, A. Tóth, P. R. Hornsby, P. A. Cusack, M. Cross, G. Marosi: XPS Analysis of Zinc Hydroxystannate-Coated Hydrated Fillers, *Surf. Interface Anal.* 34 (2002) 735.

Carbon Based Si- and Cr-containing Thin Films

Diamond-like carbon coatings owing to the combination of useful properties are gaining broadening fields of application, especially in high-tech areas. Modification of them by silicon together with different metals is in the forefront of investigations and industrial development.

Si- and Cr-containing a-C films were deposited simultaneously by dual magnetron sputtering sources onto polished silicon wafers. The chemical composition and the bonding states of the constituent elements were characterized mainly by X-ray photoelectron spectroscopy.

The surface chemical composition together with the applied RF *(red)* and DC *(blue)* power of the various samples are shown in the figure.

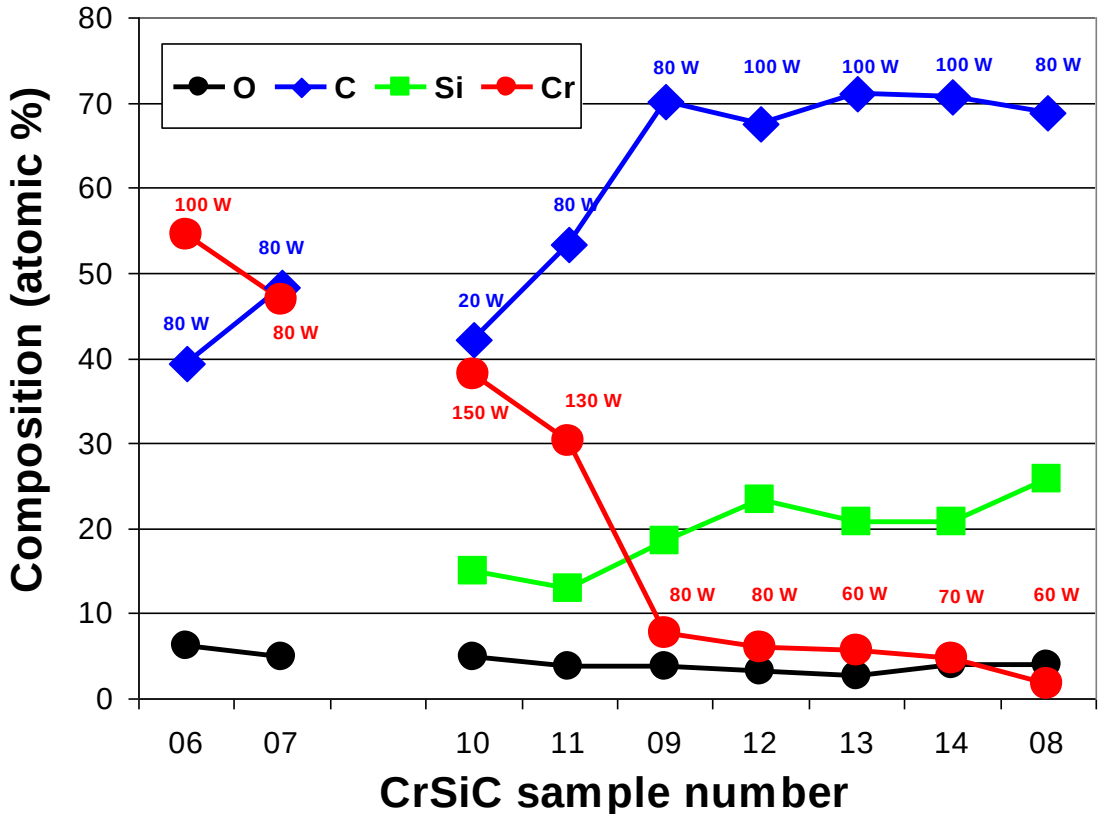

Conclusions based on the quantitative results:

- The chromium content can be controlled by the RF power of the Cr source. However, presence of the tetramethyl silane affects significantly the quantity of Cr and also C.
- The carbon content is influenced by both the DC power on C target and the addition of tetramethyl silane.
- The silicon content seems to be less affected by the applied power to targets.
- Negligible amount of oxygen was found in the films after a moderate Ar^+ ion etch at 2.5 keV for 5 min.

I. Bertóti, M. Mohai, K. Kereszturi, A. Tóth, E. Kálmán: Carbon based Si- and Cr-containing thin films: Chemical and nanomechanical properties, *Solid State Sciences* 11 (2009) 1788.

Surface Investigation of Zinc Ferrite Nanopowders

The spinel ferrites contain a close-packed cubic structure of oxygen ions in which tetrahedral (A) and octahedral (B) interstitial sites are occupied by cations. Zinc ferrite belongs to the class of normal spinels, which presumably have a cation distribution of $(Zn^{2+})_A((Fe^{3+})_2)_B(O^{2-})_4$.

Zinc ferrite nanopowders were prepared by the conventional ceramic processing from Fe_2O_3 and ZnO powders calcined in air at 900 ºC for 6 h. The product was characterised by several analytical methods.

Crystalline structure by XRD	zinc ferrite, $ZnFe_2O_4$
Bulk composition by ICP	1.00 Fe_2O_3 · 0.99 ZnO
Surface composition by XPS	1.00 Fe_2O_3 · 2.01 ZnO

The bulk and surface chemical compositions of the samples significantly differed. The XPS results indicated huge surface enrichment of ZnO. No significant chemical shift of the Zn2p doublet could be measured in the samples. To explain the surface enrichment of Zn, the following model was assumed: the spherical particles of zinc ferrite covered by a layer of ZnO. The thickness of ZnO layer was calculated from the XPS intensities by the *Layers-on-Sphere* model.

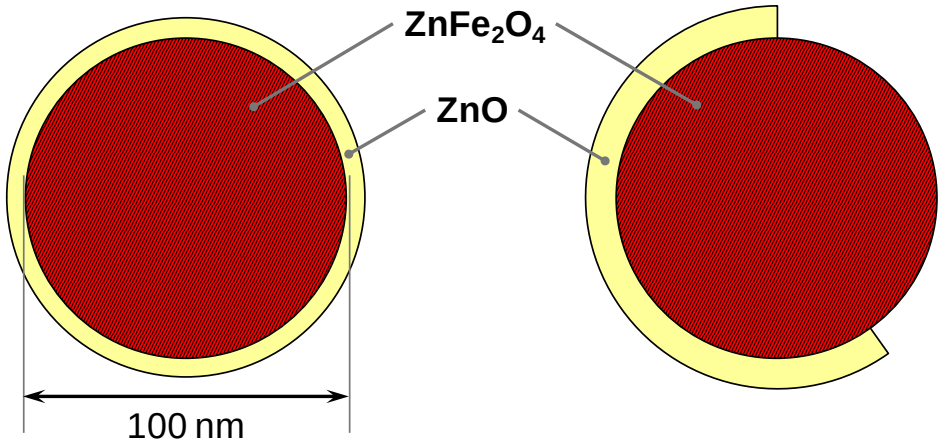

The calculated thickness of the ZnO layer was 0.16 nm. This result is unacceptable, as it is less than one monolayer (0.26 nm). Thus the model was changed to *Islands-on-Sphere*, and the thickness of the ZnO layer was fixed to 0.26 nm. The calculated coverage was 65%. These results revealed that the “huge” zinc surplus was only slightly more than half of a monolayer.

Obviously, it does not mean that the ZnO forms a sharp layer on the ferrite particle but it helps to estimate the real quantity of the surplus by transforming to concentration data into other dimension.

I. Mohai, J. Szépvölgyi, I. Bertóti, M. Mohai, J. Gubicza, T. Ungár: Thermal Plasma Synthesis of Zinc Ferrit Nanopowders, *Solid State Ionics* 141-142 (2001) 163.

Rough Surfaces: Application of Polyhedral Model

Samples with rough surfaces, covered by thin overlayers, commonly occur in practice. Examples include microcrystalline samples, grains, grooved surfaces, microelectronic devices, etc. The rough surfaces with macroscopic or microscopic structures can be modelled by small planar units at different angles, i.e., facets of one or several types of polyhedra.

Silicon atomic force microscopy standard sample, one dimensional array of triangular steps with precise linear and angular sizes in the micrometer range, covered by native oxide layer was measured (type TGG1, NT-MDT Co.). The flat and patterned areas of the sample were selected by masking with Al foil.

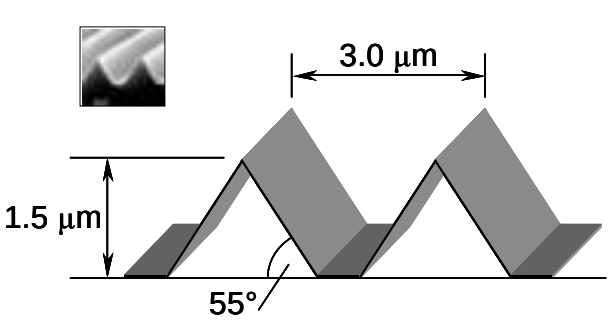

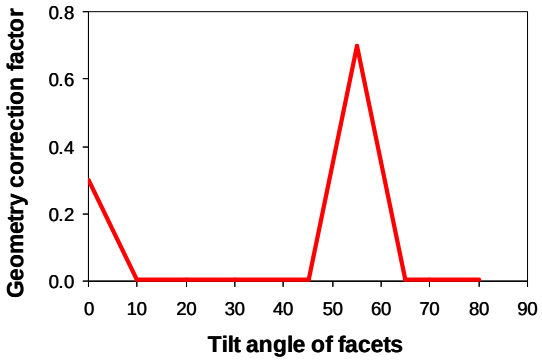

The parameters of the *Layers-on-Polyhedron* model (the tilt angles of the facets together with their corresponding relative projected areas) were based on the sample geometry specified by the manufacturer.

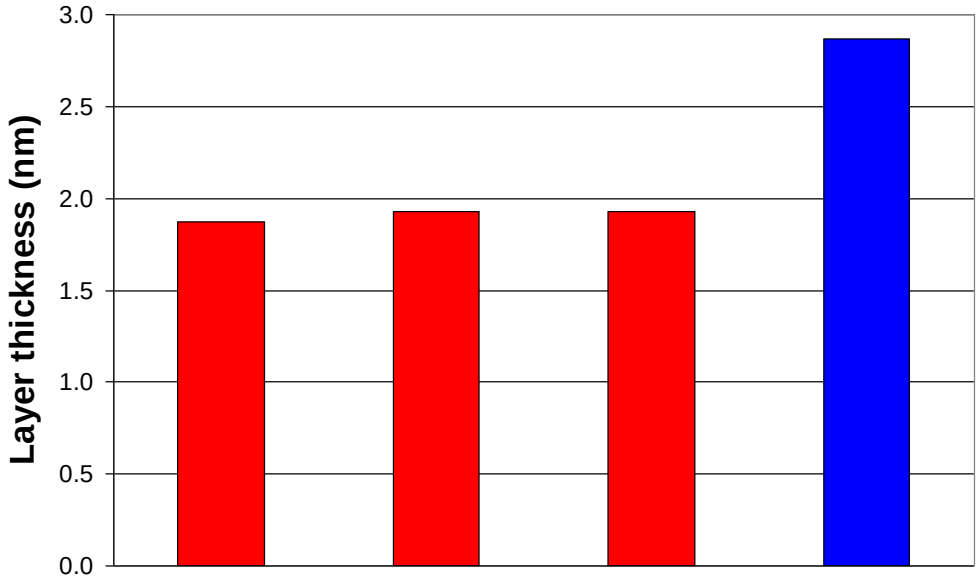

Sample shape	flat	flat	roof	roof
Quantification model	planar	planar	polyhedral	planar
Spectrum mode	FAT	FAT, 60°	FAT	FAT

The thickness values of the SiO_2 layer, measured on the flat and patterned parts of the sample, are in excellent agreement, while when a simple planar model is applied to calculate thickness from data measured on patterned samples, the layer thickness is overestimated by nearly 50 %. The larger is the ratio of the facets with higher tilt angles, the larger is the difference.

M. Mohai: Calculation of Layer Thickness on Rough Surfaces by Polyhedral Model,
Surf. Interface Anal. 40 (2008) 710.

Boron Nitride Coating on Multiwall Carbon Nanotube

Growing attention has been paid to the application of multiwall carbon nanotubes into various ceramic matrixes to improve their mechanical properties and also to increase their thermal and electrical conductivity. However, application of nanotubes is limited because of their ability to react with oxygen at high temperature. Coating them with boron nitride is one of the possibilities to maintain the advantage of using the carbon nanotubes, but to avoid the thermal degradation during the sintering process or on the high temperature applications.

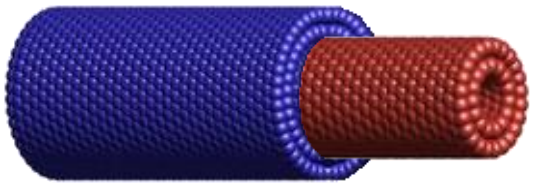

Boron nitride coating Carbon nanotube

Thin boron nitride films were deposited onto outer surfaces of multiwall carbon nanotubes, with various diameter and wall thickness, by dip coating, which involves infiltration by boric acid solutions and subsequent nitridation of the boron oxide in ammonia flow at 1050 °C.

Samples were characterized by X-ray photoelectron spectroscopy for surface composition and BN coverage. The thickness of the BN coatings was calculated by *Layers-on-Nanotube* model based on XPS intensities.

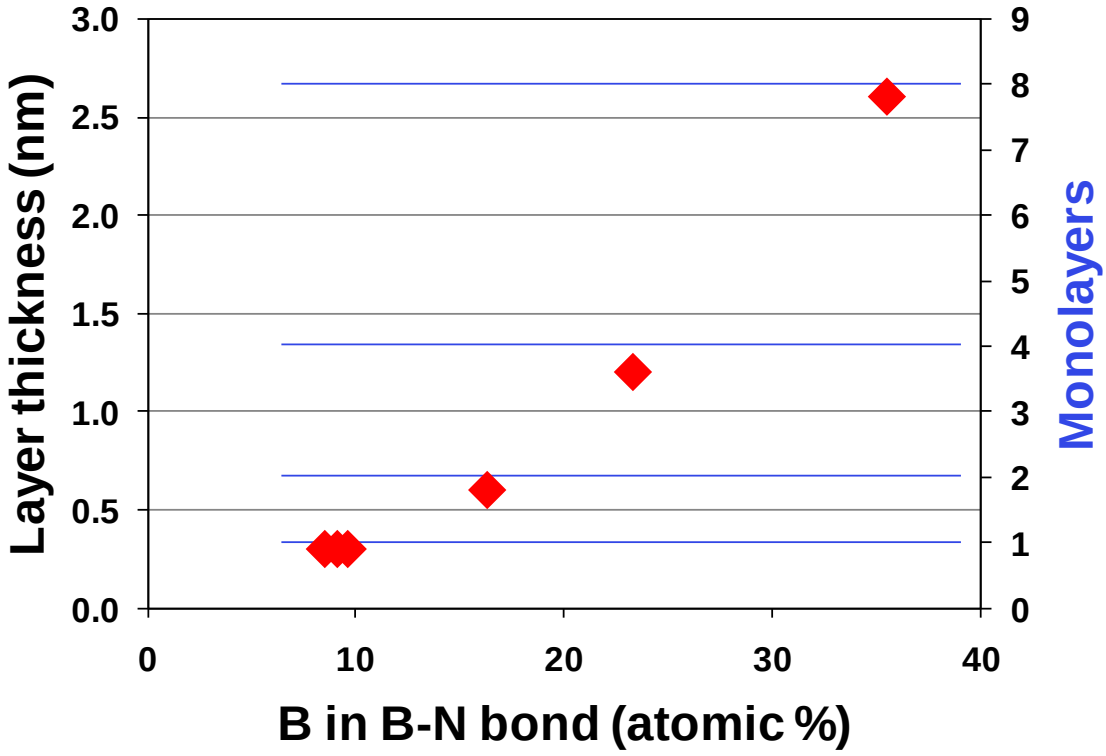

The thickness of the layers are increasing with the increasing boron content. Although these measurements supply only average results, the calculated layer thickness values are quite close to the multiple of the monolayer thickness of the boron nitride (0.33 nm).

M. Mohai, I. Mohai, Z. Sebestyén, A. Gergely, P. Németh, J. Szépvölgyi: Surface Characterisation of Boron Nitride Layers on Multiwall Carbon Nanotubes, *Surf. Interface Anal.* 42 (2010) 1148.

Composite Underfloor Heating Pipe *(Case Study)*

The manufacturer of the polyethilene–aluminium–polyethilene composite underfloor heating pipe complained at the supplyer of the aluminum ribbon (used to form the aluminium inner tube) because at some parts of the pipe the composite layers were split, i.e., the polyethilene tubes separated from the aluminium one at bending the composite tubes. These separated faulty surfaces were highly hydrophobic.

The XPS investigation of the Al ribbons discovered that the hydrophobic spots contained silicon while on the intact places no Si could be detected, as demonstrated in the figure. The chemical state of Si corresponded to the one of the dimethyl siloxane.

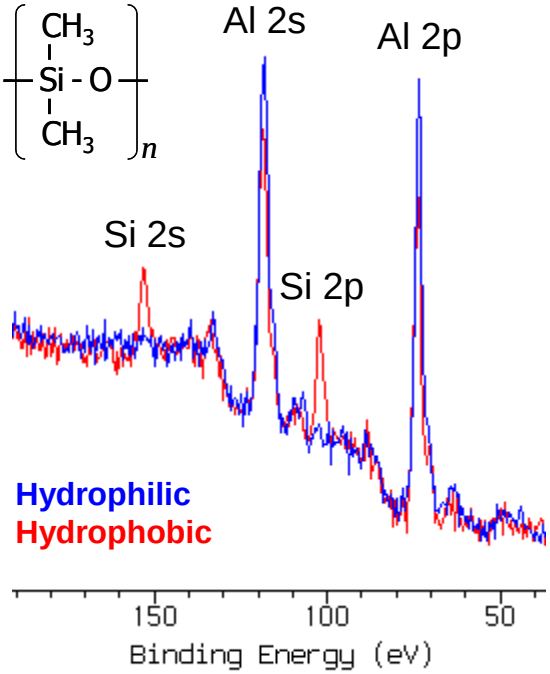

The manufacturer started to hunt for the potential sources of the silicon.

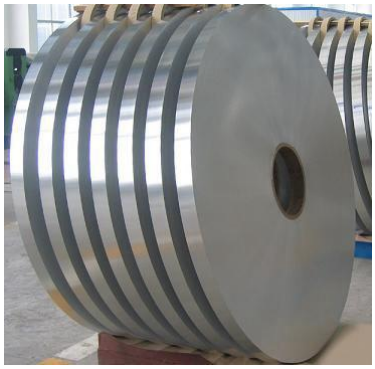

In the factory the aluminium is rolled to sheet, the large spool of sheet is cut into reels of stripes. No silicon containing oil or other lubricant is used.

Then the reels of stripes are heat treated at about 300 °C. The end of the reels is fixed with a piece of adhesive tape. A few days before producing the faulty batch, a new type of adhesive tape was introduced. It turned out, that the silicon containing polymer of the tape was the source of the contamination!

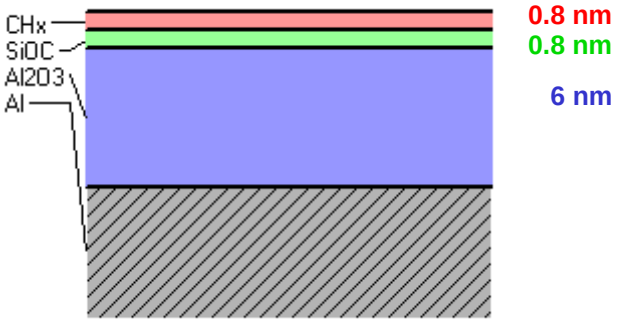

The thickness of the siloxane layer in the spots, calculated by the *Layers-on-Plane* model, was only 0.8 nm but it was enough to damage thousand of meters of aluminium ribbon.

I. Bertóti, M. Mohai: Alumínium szalagok felületvizsgálata röntgen-fotoelektron spektroszkópiával.
(Surface Investigation on Al Ribbons by X-ray Photoelectron Spectroscopy.)
Research report (unpublished).

Contact

The author would be indebted if you send him comments and suggestions on further development of the program. Reports on errors of library data (possibly with the suggested new value) and program bugs are also accepted. Reprints of papers (electronic or printed) referring to XPS MultiQuant are highly appreciated.

Dr. Miklós Mohai
Institute of Materials and Environmental Chemistry
Research Centre of Natural Sciences

E-mail: mohai.miklos@ttk.hu
Web: http://aki.ttk.hu/XMQpages/XMQhome.php
ORCID: 0000-0002-5162-1590